RADC-TDR-62-75
ASTIA Document No.

THE UNIVERSITY OF MICHIGAN

THEORETICAL AND EXPERIMENTAL INVESTIGATION OF LARGE-SIGNAL TRAVELING-WAVE TUBES

QUARTERLY PROGRESS REPORT NO. 6

Period Covering October 1, 1961 to January 1, 1962

ELECTRON PHYSICS LABORATORY

Department of Electrical Engineering

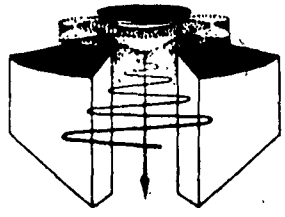

By: C. A. Brackett
S. K. Cho
G. T. Konrad
S. G. Lele
Y. C. Lim
R. J. Martin
J. E. Rowe
C. P. Wen

Approved by: J. E. Rowe

January, 1962

CONTRACT WITH:
THE ROME AIR DEVELOPMENT CENTER, GRIFFISS AIR FORCE BASE, NEW YORK. DEPARTMENT OF THE AIR FORCE PROJECT NO. 5573, TASK NO. 557303, CONTRACT NO. AF30(602)-2303.

OFFICE OF RESEARCH ADMINISTRATION · ANN ARBOR

RADC TDR-62-75

THE UNIVERSITY OF MICHIGAN
ANN ARBOR, MICHIGAN

QUARTERLY PROGRESS REPORT NO. 6

FOR

THEORETICAL AND EXPERIMENTAL INVESTIGATION OF LARGE-SIGNAL TRAVELING-WAVE TUBES

This report covers the period October 1, 1961 to January 1, 1962

Electron Physics Laboratory
Department of Electrical Engineering

By: C. A. Brackett
S. K. Cho
G. T. Konrad
S. G. Lele
Y. C. Lim
R. J. Martin
J. E. Rowe
C. P. Wen

Approved by: J. E. Rowe
J. E. Rowe, Director
Electron Physics Laboratory

Project 03736

CONTRACT NO. AF30(602)-2303
DEPARTMENT OF THE AIR FORCE
PROJECT NO. 5573, TASK NO. 557303
PLACED BY: THE ROME AIR DEVELOPMENT CENTER
GRIFFISS AIR FORCE BASE, NEW YORK

January, 1962

ABSTRACT

Detailed experimental data on an S-band high-power traveling-wave amplifier with a variable-pitch helix is presented with particular emphasis on the efficiency enhancement achieved across the frequency band. Efficiency improvement factors of from 1.4 to 2 to 1 are demonstrated. The gain is also enhanced over the entire frequency band of operation.

Experimental data on a new elliptic cavity coupler for use with a helical circuit is shown. Low VSWR and insertion loss over a broad frequency band are indicated.

The design of a magnetron injection gun for use with a high-power amplifier is outlined.

Additional details on the noise transport analyses and beam-plasma interaction theory are given.

TABLE OF CONTENTS

LIST OF ILLUSTRATIONS

LIST OF TABLES

PERSONNEL

Scientific and Engineering Personnel		Time Worked in Man Months*
W. Dow	Professors of Electrical Engineering	.06
G. Hok		1.06
J. Rowe		.18
C. Dolph	Professor of Mathematics	.48
C. Yeh	Associate Professor of Electrical Engineering	.63
G. Konrad	Associate Research Engineers	1.37
L. Paul		.55
S. Cho	Assistant Research Engineers	.93
H. Detweiler		.86
H. Krage		2.65
S. Lele		1.44
Y. Lim		2.46
R. Martin		1.34
C. Wen		2.76
J. Kurtz	Research Assistants	1.06
J. Mason		.72
S. Salinger		.51
G. Burklund	Assistants in Research	.25
J. Connolly		.59
T. DeMassa		.51
L. Kistler		.31
J. Loh		1.47
A. Pajas		2.03
D. Sinnett		1.55
D. Steele		.33
D. Terry		.55
D. Wright		.27
K. McCrath	Electronics Technician	.30
C. Murillo	Circuits Technician	.13
Service Personnel		
V. Burris	Assistant to Director	.81
T. Knopf	Shop Foreman	.55

Service Personnel (cont.)		Time Worked in Man Months*
R. Casterline	Instrument Makers	.81
M. Ellicott		1.23
E. Kayser		.37
M. Prince		1.60
M. Tobias		.25
H. Wagner		.04
F. Wisniewski		1.44
R. Kepler	Machinist	.90
W. Bowen	Assembly Technicians	.46
J. Kelly		2.46
J. Murphy		.13
M. Otto		.46
M. Potes		.93
G. Beauchamp	Draftsman	.65
J. Corkin	Secretaries	.79
P. Foerster		.79
J. Smith		.34

* Time Worked is based on 172 hours per month.

ARTICLES PUBLISHED DURING THE LAST QUARTER

G. Hok, "Conservation Principles in Multivelocity Electron Flow", Trans. IRE-PGED, vol. ED-8, No. 6, pp. 452-461; November, 1961.

QUARTERLY PROGRESS REPORT NO. 6

FOR

THEORETICAL AND EXPERIMENTAL INVESTIGATION OF

LARGE-SIGNAL TRAVELING-WAVE TUBES

1. Purpose

The purpose of this study is to investigate theoretically and experimentally the operation of large-signal traveling-wave tubes. Specifically it is planned to investigate r-f structures for high-power tubes, electron injection systems of both the solid- and hollow-beam types, and means for improving the interaction efficiency. The topics to be studied under the project are continuations of work reported under Contract No. AF30(602)-1845.

2. Objectives for the Period (J. E. Rowe)

2.1 Nonlinear Interaction Analysis. During this period the two-dimensional nonlinear integro-differential equations for the traveling-wave tube and the klystron were to be programmed for solution on the IBM-709 digital computer.

2.2 Variable-Pitch Helix Tubes. Further experimental data on the variable-pitch helix amplifier with a 50 percent phase velocity variation was to be taken. Also initial experimental cold-test work on a helix with a 70 percent phase velocity variation was to be carried out.

2.3 Uhf Crestatron. During this quarter further testing of the uhf Crestatron was to be made with a metallic shield around the slow-wave structure.

2.4 Poisson Cell for Axially Symmetric Electron Gun Design. During this quarter further design work on the $P_\mu = 1$ gun was programmed as well as initial work on the $P_\mu = 2$ gun.

2.5 Noise Transport in Linear-Beam Devices. It was planned to continue programming both the Monte Carlo analysis and the density function analysis of noise transport in linear beams for solution on a digital computer.

2.6 Beam-Plasma Interaction Theory. Further work was planned on obtaining the dispersion equation for a beam-plasma interaction accounting for collision terms. In particular closed form solutions are sought.

3. Two-Dimensional Nonlinear Interaction Theory for Klystrons and Traveling-Wave Amplifiers (J. E. Rowe)

In the previous progress report the general two-dimensional nonlinear interaction equations for klystrons and TWA's were derived following the method previously used to derive the one-dimensional equations. The two-dimensional expression for the space-charge potential was obtained from the appropriate Green's function for ring charges of thickness dr' and dz'.

The nonlinear equations have been transformed into difference form and have been partially programmed for solution on an IBM-709 digital computer. They are quite complicated and in order to conserve computation time considerable effort is being devoted to program optimization in writing the computer program.

The space-charge-force integrals contain infinite summations of Bessel functions and thus are time consuming to compute. In fact each space-charge integral must be evaluated $6(32)^2$ times at each integration

plane along the tube when 6 beam subdivisions are considered with 32 electrons per ring of charge. These infinite sums have been programmed and calculated for specific values of $\gamma a'$ and $\gamma b'$. It is planned to synthesize polynomials by a least squares method to fit the calculated functions in order to materially reduce the required computation time.

During the next period the digital computer programming and check out will be completed. Also representative space-charge-force weighting functions will be computed using both the infinite series method and the polynomial method.

4. Experiments on Variable-Pitch Helix Traveling-Wave Tubes

(J. E. Rowe, C. A. Brackett)

4.1 Introduction. In order to test the variable-pitch traveling-wave amplifier at higher power levels, new and improved coupled-helix couplers were designed. These couplers increase the bandwidth so that the tube operates over most of the frequency regime from 2.0 to 4.0 Gc. The attenuation used for stability in this tube is obtained from a coupled-helix attenuator in which the coupler wire is embedded in lossy ceramic material. The position of the attenuator along the helix is adjustable during operation.

The tube was tested under two basically different conditions: first, the coupled-helix couplers were placed over the uniform-pitch region and gain and power output measurements were made; and second, the couplers were moved so that the output coupler was over the variable-pitch region and gain and power output were again measured. For some tests the attenuator position was held constant while the voltage was optimized at each frequency. For other tests the attenuator position was also optimized. The purpose of these different tests was

to shed some light on the criticality of the location of the tapered section of the helix. The results will be evident in the data to be presented. The location of the start of the taper is not unduly critical.

In testing, the beam voltage and attenuator position were set in a manner to maximize the small-signal gain and then the power output was recorded as the power input was varied from low levels to as close to saturation as possible. It was not always possible to saturate the tube with the available drive power. At the saturation power level, or the highest available input power if the tube would not saturate, the beam voltage and attenuator position were again varied to yield the maximum power output. This procedure was followed for both the uniform- and variable-pitch sections at each frequency.

4.2 Experimental Results. The amplifier efficiency is shown in Fig. 4.1 for both the uniform-pitch and variable-pitch tests with the attenuator position held fixed. It is seen that a substantial improvement in the efficiency is obtained over the entire operating band with the variable-pitch tube. The improvement factor varies from 1.4 to 2.0. Since it was not possible to saturate the tube at each frequency, due to the lack of drive, the data are presented for a constant input drive of one watt.

The gain vs. frequency is shown in Fig. 4.2 along with efficiency data when both the voltage and attenuator position are optimized for maximum power output. The gain at one watt of drive is seen to be greater for the variable-pitch tube than for the uniform-pitch tube. This is attributed to the fact that, because of the phase focusing provided by the variable phase velocity circuit, more of the beam current,

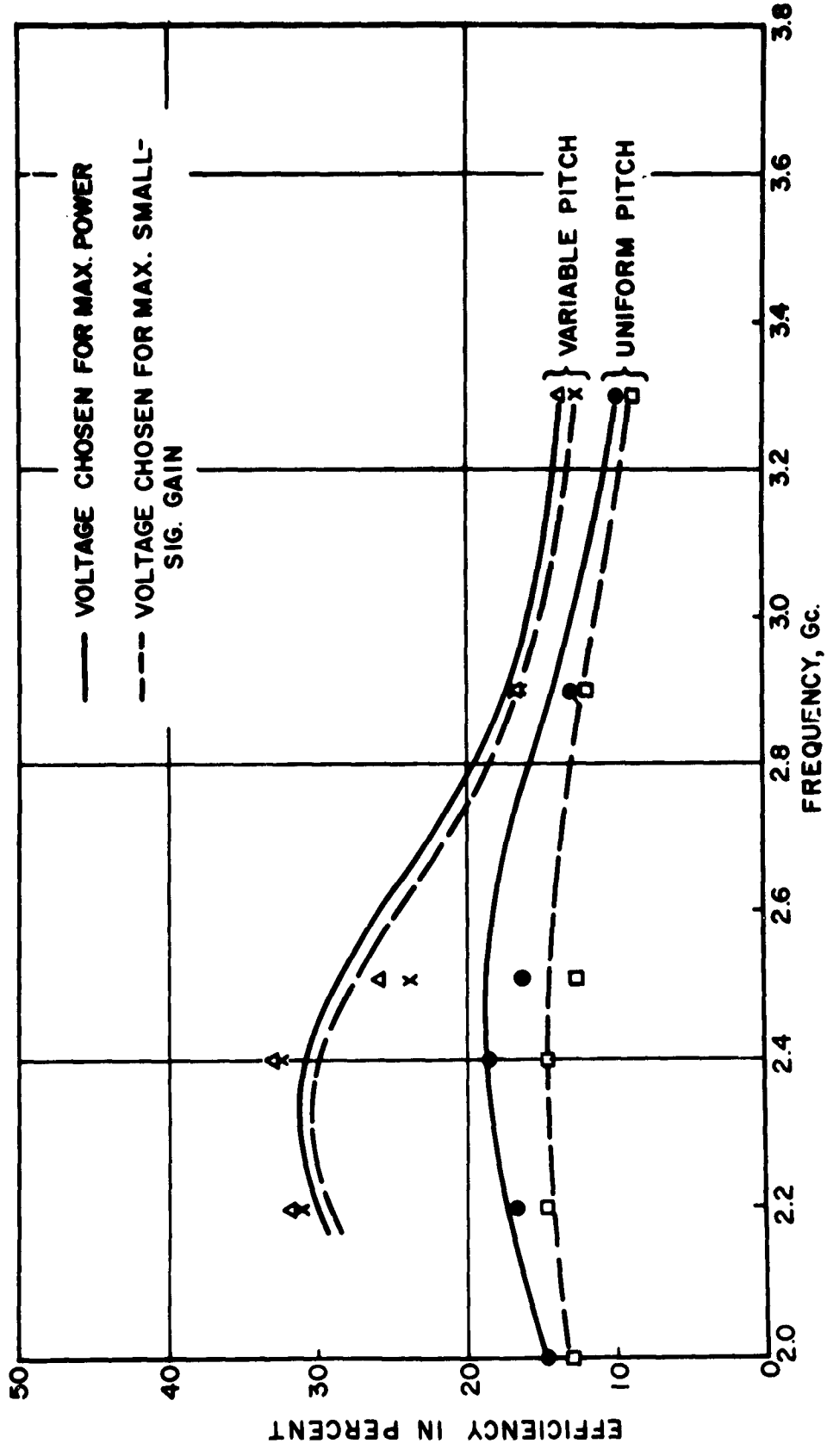

FIG. 4.1 CONVERSION EFFICIENCY OF EXPERIMENTAL S-BAND HELIX TWA BEFORE AND AFTER TAPERING ($C \approx 0.1$, $QC \approx 0.2$, $V_o \approx 3600$ VOLTS, P_o(MAXIMUM) $\approx$ 200-400 WATTS).

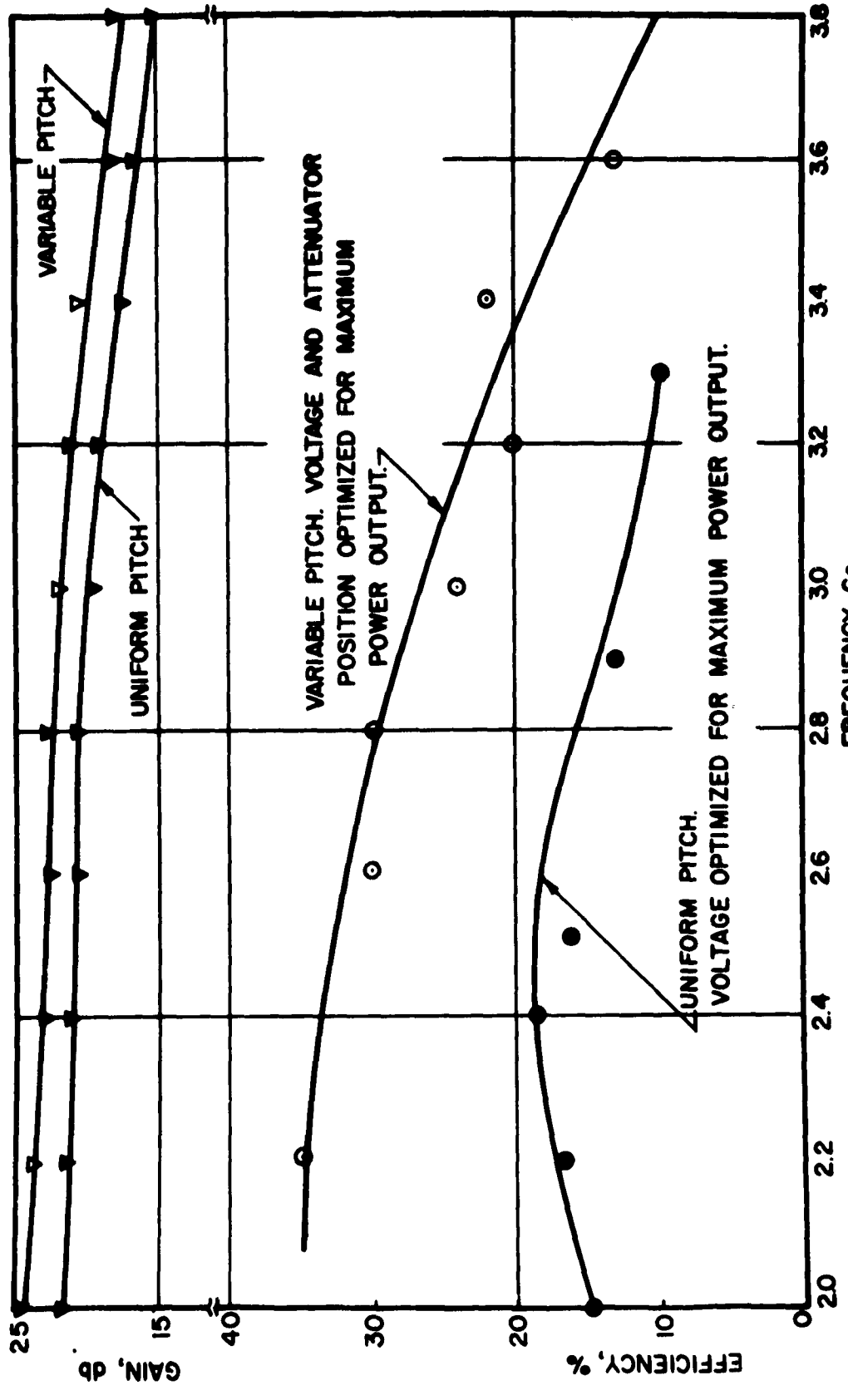

FIG. 4.2 MAXIMUM EFFICIENCY AND SMALL-SIGNAL GAIN VS. FREQUENCY BEFORE AND AFTER TAPERING (DRIVE LEVEL = 1 WATT).

in particular the beam core, is coupled to the circuit, thereby increasing the gain parameter. The improvement at both large- and small-signal levels is approximately 3 db and is uniform over the frequency band.

The variable-pitch helix tube showed less gain compression at high power levels and the beam voltage for maximum power output was consistently closer to the beam voltage for maximum small-signal gain than for the uniform-pitch helix tube.

4.3 Program for Next Period. During the next period experimental data will be taken at input power levels sufficient to saturate the amplifier over the frequency band. In addition cold test data will be taken on a new tube with a phase velocity variation of 70 percent.

5. Beating Wave Klystron (G. T. Konrad)

At the end of the last quarter, testing on the beating-wave klystron was started. The tube consists of two sections of helix separated by a solid cylindrical drift tube. A photograph is shown in Fig. 5.1. The beam is bunched in the first section and then drifts through the cylindrical drift tube as in a klystron. Then as the beam enters the second helix section the signal is introduced in the right place and with the proper phase for best interaction.

In essence then the signal interacts with a prebunched beam. This would mean that by neglecting the length used for prebunching the beam the interaction length for the tube should be considerably shorter. It would also be reasonable to expect a higher efficiency.

During the testing of this tube it was found that the gain per unit length did indeed increase significantly. In the particular case considered here, where the interaction length was in the vicinity of 2

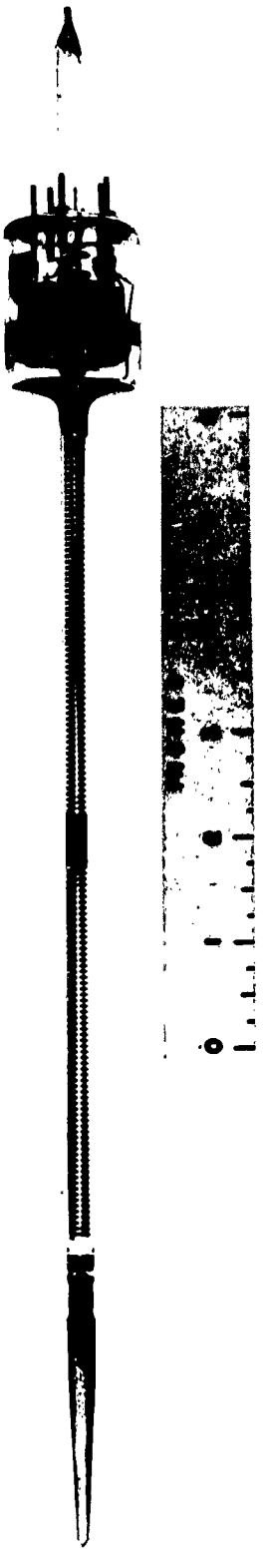

FIG. 5.1 BEATING-WAVE KLYSTRON.

to 3 inches, an increase in small-signal gain of about 10 db was observed. Figure 5.2 shows some preliminary data to substantiate this. It should be mentioned that the degree of prebunching as well as the phase was optimized for maximum gain at each frequency. For comparison a curve is shown on the same graph for no prebunching.

The increase in efficiency was not nearly as significant as that in the small-signal gain. It is not possible to give specific data and graphs at this time because the r-f testing of this tube is not yet complete. During the next quarter testing of this tube is expected to be finished so that detailed results will be available.

6. Elliptic Cavity Couplers for Traveling-Wave Tubes (G. T. Konrad, S. K. Cho)

Some time ago Professor G. Hok suggested the use of the elliptic cavity as a circuit for the microwave voltage tunable magnetron where the oscillator tube is placed at one focus of the ellipse and the load at the other focus. This scheme worked successfully and in fact the oscillator power output was nearly constant over one octave bandwidth at S-band. Recently Professor J. Rowe suggested the use of the elliptic cavity as a transducer from either a coaxial line or waveguide to a helical r-f structure. A perspective view of the coupler and helix is shown in Fig. 6.1.

If a cylindrical cavity of elliptical cross section is considered then, according to geometrical optics, all reflections from the cavity walls serve to converge energy from one focus of the ellipse to the other. This holds exactly for waves of all frequencies which have their electric and magnetic vectors transverse to the plane of the elliptic cross section (TEM modes). By placing an antenna at one focus

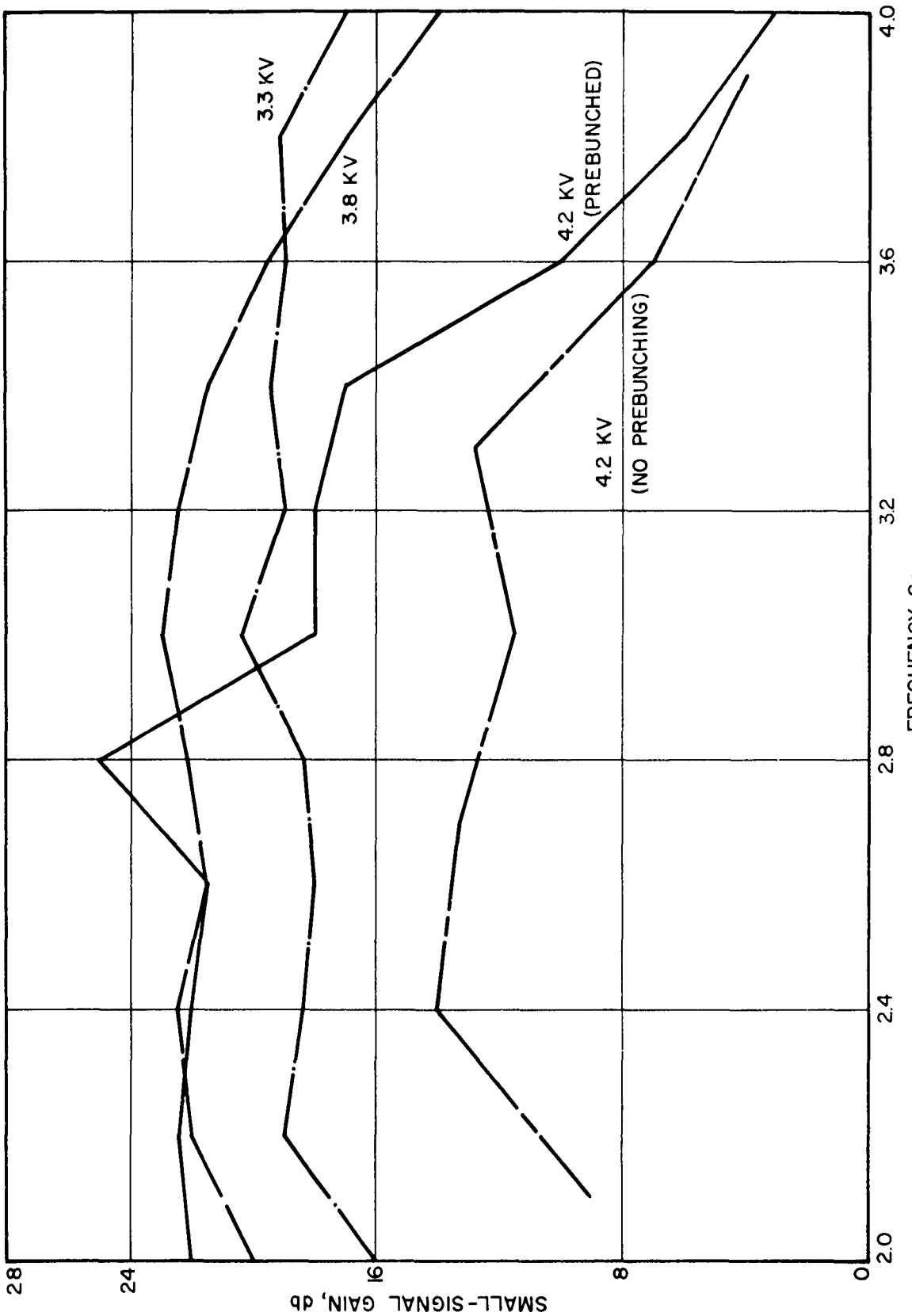

FIG. 5.2 SMALL-SIGNAL GAIN FOR THE S-H Y-4 BEATING-WAVE KLYSTRON.

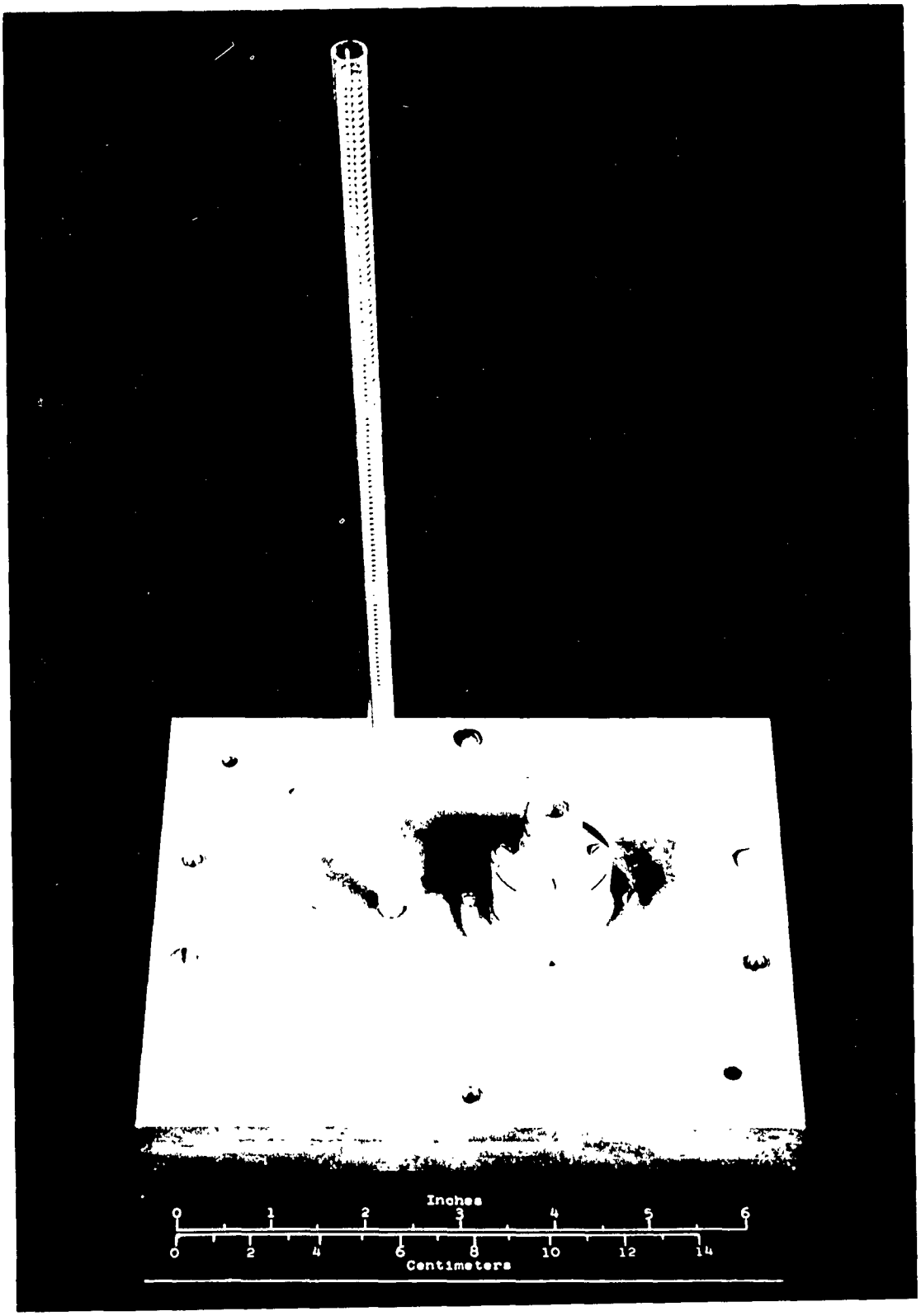

FIG. 4.1 PERSPECTIVE VIEW OF THE ELLIPTIC CAVITY USED AS THE REFLEX.

and a nonreflecting load at the other, there would be no spurious reflections and broadband operation would be obtained.

The zero order radial wave in an elliptic cavity is a TEM wave so that neither the electric nor magnetic field has a component in the direction of propagation. The reflected wave from the cavity wall must also be a simple wave and hence as long as the minimum distance from a point of reflection to one of the focal axes is greater than a quarter wavelength, very little distortion of the reflected wave should occur. It is this distance which is important in terms of the low frequency cutoff, and it should enter into bandwidth considerations. In general the distance from either focus to the cavity wall should be large compared to one quarter of the cutoff wavelength since high currents flow in the cavity walls and hence losses will be high. This should enter into insertion loss considerations. The height of the cavity is of course determined from impedance-match considerations.

A theoretical analysis of a waveguide with an elliptical cross section was originally made by L. J. Chu[1]. The present investigation on the elliptical cavity as a radial nonuniform waveguide is based on Chu's theoretical work. VSWR and insertion loss of two cavities with different dimensions were determined for the S-band region.

For the transition from a coaxial line to the cavity, a cone[2] is used which is situated at one of the foci of the cavity. This is illustrated in the cross section drawing of Fig. 6.2. An S-band helix as a cavity-termination occupies the other focal point of the ellipse.

---

1. Chu, L. J., "Electromagnetic Waves in Elliptic Hollow Pipes of Metal", Jour. Appl. Phys., vol. 9, No. 9, pp. 583-591; September, 1938.
2. Adachi, S., "A Theoretical Analysis of Semi-Infinite Conical Antennas", Trans. IRE, vol. AP-8, No. 6, pp. 534-537; November, 1960.

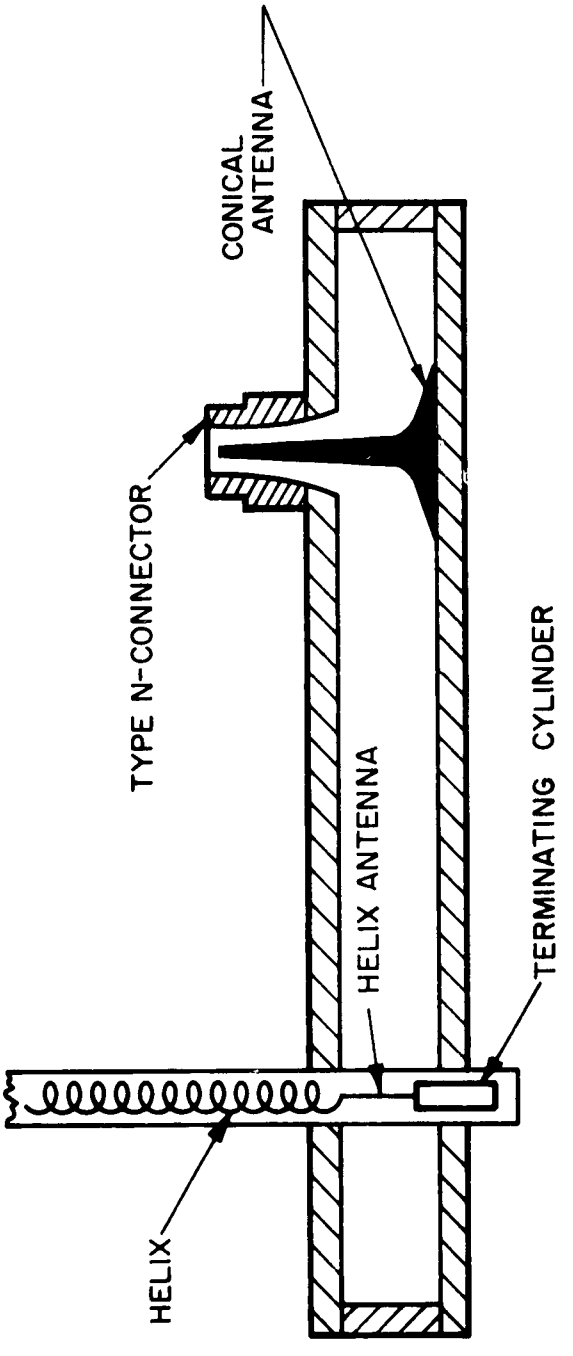

FIG. 6.2 SECTION VIEW OF ELLIPTIC CAVITY.

It may be observed that an elliptical cavity, because of its inherent broadband property, might be used as a waveguide device in any frequency region, insofar as the physical construction of the cavity is feasible. Though the present work shows some experimental results only in the S-band region, a further investigation is presently underway in the X-band region. Data obtained so far appear to confirm the above belief.

Measurements of VSWR and insertion loss for two different cavities are shown in Figs. 6.3 and 6.4, respectively. As shown in Fig. 6.3 the cavity of smaller dimension exhibits a cutoff phenomenon in the neighborhood of 2.4 Gc, which conforms to Chu's theoretical results. The larger cavity is designed to bring the cutoff point down to below 2.0 Gc. The larger cavity had major and minor axes of 4.75 and 4.50 inches, respectively, while the smaller cavity had major and minor axes of 4.00 and 3.46 inches, respectively.

The insertion loss for both cavities seems to be a bit high; this may probably be ascribed to rough machine work of the cavity. No deliberate efforts for minimization of the insertion loss were made.

The helix, as a cavity termination, is provided with a straight wire antenna at one end, which, in turn, is short-circuited by a cylindrical sleeve. The antenna length had to be adjusted for optimum VSWR. It has been experienced in this work that the helix antenna length and its relative position in the cavity are rather critical factors in obtaining a good VSWR in the cavity.

During the next period work will be continued on the X-band elliptic cavity coupler both with coaxial-line and waveguide outputs.

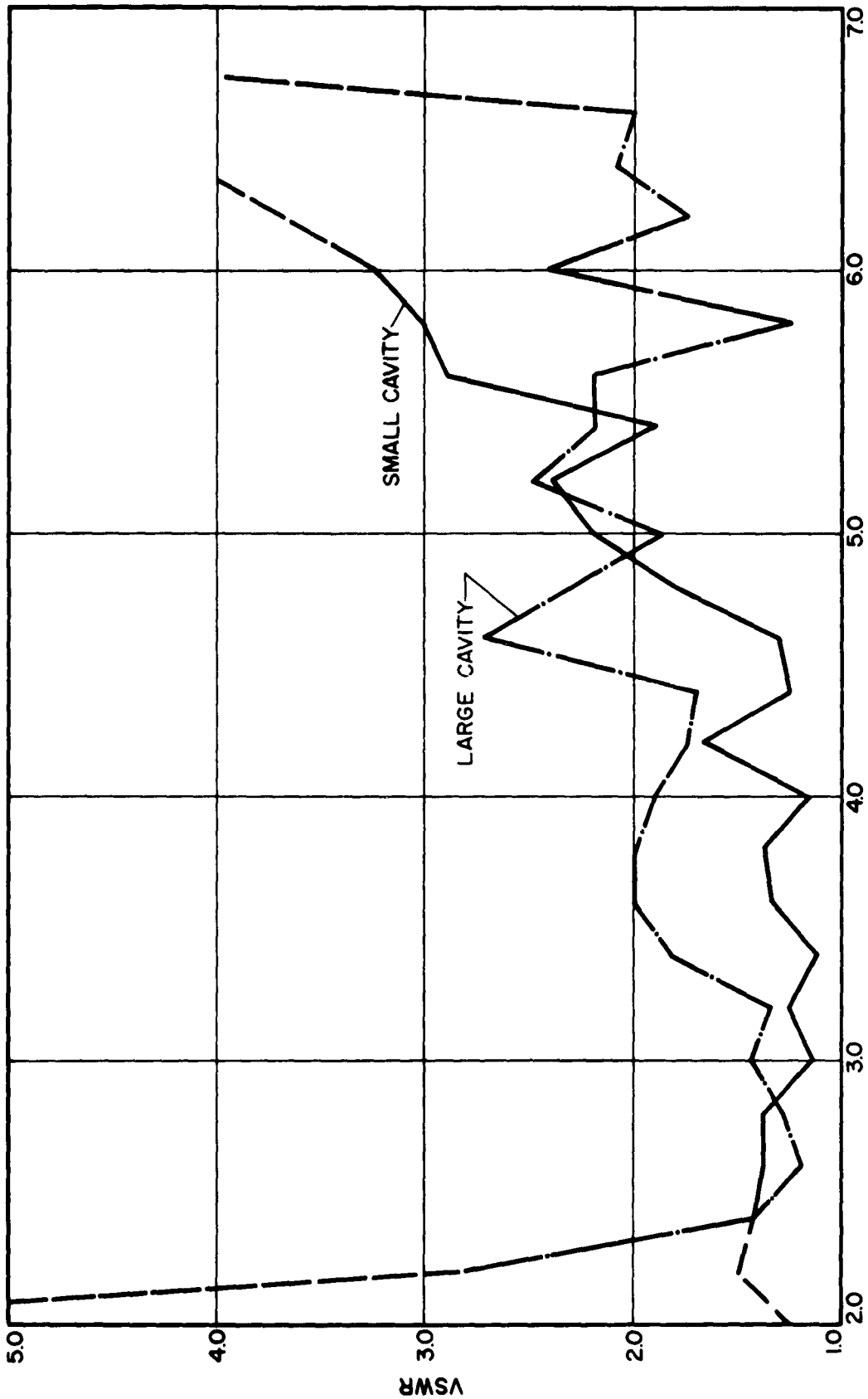

FIG. 6.3 ELLIPTIC CAVITY VSWR FOR TWO DIFFERENT CAVITIES.

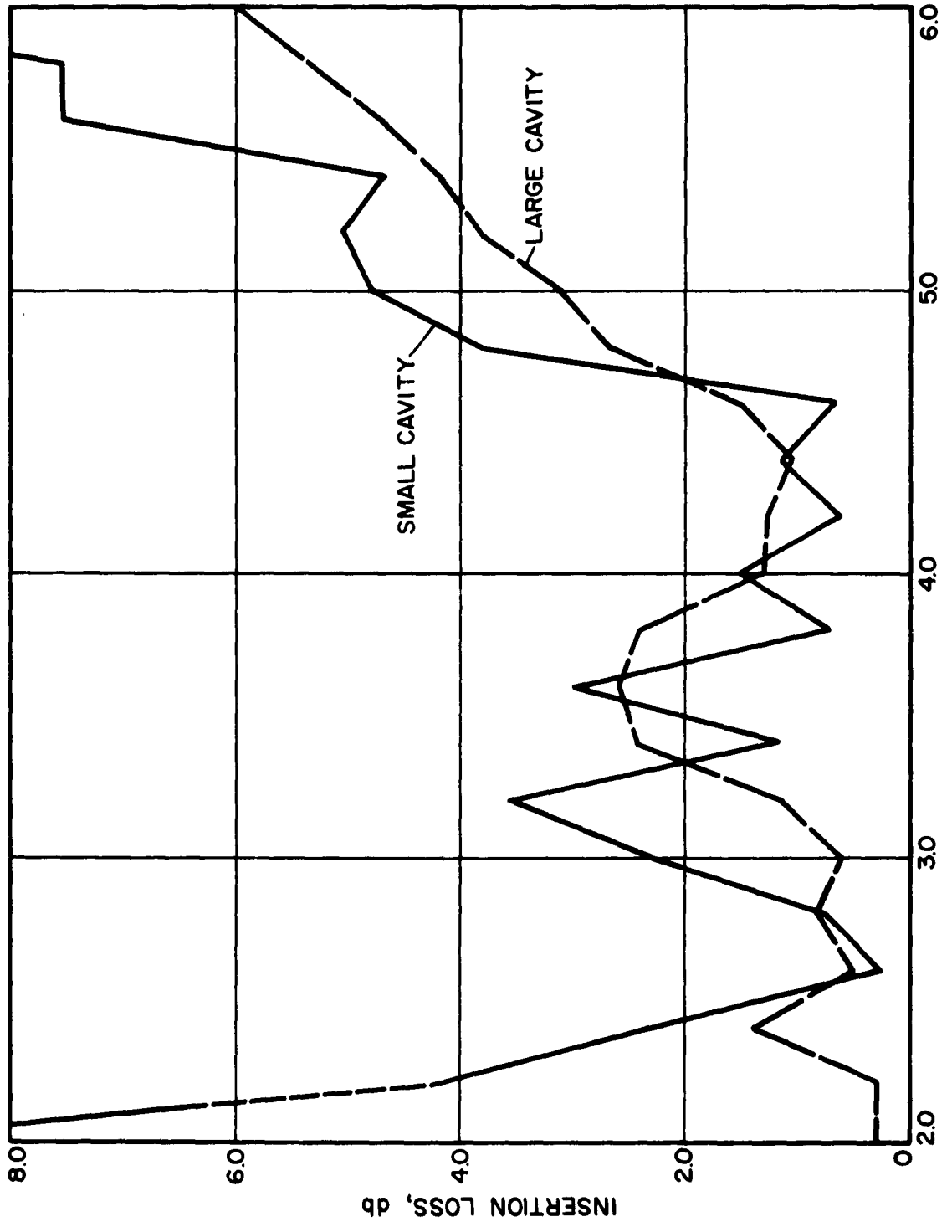

FIG. 6.4 ELLIPTIC CAVITY INSERTION LOSS FOR TWO DIFFERENT CAVITIES.

7. Uhf Crestatron (G. T. Konrad)

It was expected that during the past quarter the testing of the UHF-4 could be completed. R-f test results for an unshielded helix were reported in the last progress report. Similar results were to be given in this report, but the cathode emission dropped very markedly during testing early during this quarter. In order to obtain the required beam power in this tube, it was necessary to operate with a cathode loading of 10 amp/cm^2. This is approximately the limit for a Phillips type-B cathode, and it can be achieved with a cathode temperature of 1200°C or a little higher. It was therefore not surprising that the cathode decreased in activity after some time of operating under these conditions.

As no more cathodes were in stock it was necessary to order some from the vendor. A change was also made from type B to type S. This should permit the cathode to be operated at a lower temperature for the same current density. The new cathodes have been received recently and the UHF-4 will be rebuilt incorporating one of the type-S cathodes.

When the tube is rebuilt another interesting aspect will be investigated. As was shown in the last progress report the operating bandwidth of the UHF-4 was at least 3:1 with a relatively flat response. This feature should permit analysis of harmonics under a wide variety of drive conditions. If the tube is operating with a signal near the low frequency end, it is possible to analyze the second and third harmonics. A knowledge of this information would be useful to systems engineers. The harmonic content of the tube output will be analyzed under various drive conditions as soon as the tube is rebuilt.

8. Poisson Cells and Gun Design (R. J. Martin, S. G. Lele)

8.1 Introduction. During this quarter the effect of the use of surface electrodes with the $P_\mu = 1$ Poisson cell was studied. Ideally, the electrodes should be embedded in the wedge so that the proper potential distribution (consistent with the electrode geometry) occurs throughout the thickness of the cell. Due to a need for flexibility in determining the electrode configuration for electron gun design, surface electrodes are used to determine the potential distribution. The surface electrodes produce error in the proper potential distribution, the error increasing with thickness of the volume conducting material. The following is a discussion of the effect of the use of surface electrodes.

8.2 Procedure. The desired electron gun geometry for a $P_\mu = 1$ gun was first simulated by the use of bronze finger stock weighted by brass blocks. Due to the bulkiness of these electrodes the entire gun geometry could not be completely simulated. Also the microperveance-one cell was not constructed to allow for simulating the gun electrode geometry at the bottom surface of the Poisson cell. This is being done on later Poisson cells by shorting out current source injection points at the proper geometry. The space-charge-free potential distribution for the electron gun under study is shown in Fig. 8.1.

The next step was to better the simulation of the surface electrode geometry by the use of aluminum foil. The foil was taped to the surface of the cell with the configuration of the electron gun geometry. The brass electrodes were used to press the foil against the wedge and insure good contact with it. The use of the foil insured the simulation of the exact electrode geometry upon the wedge surface but still did

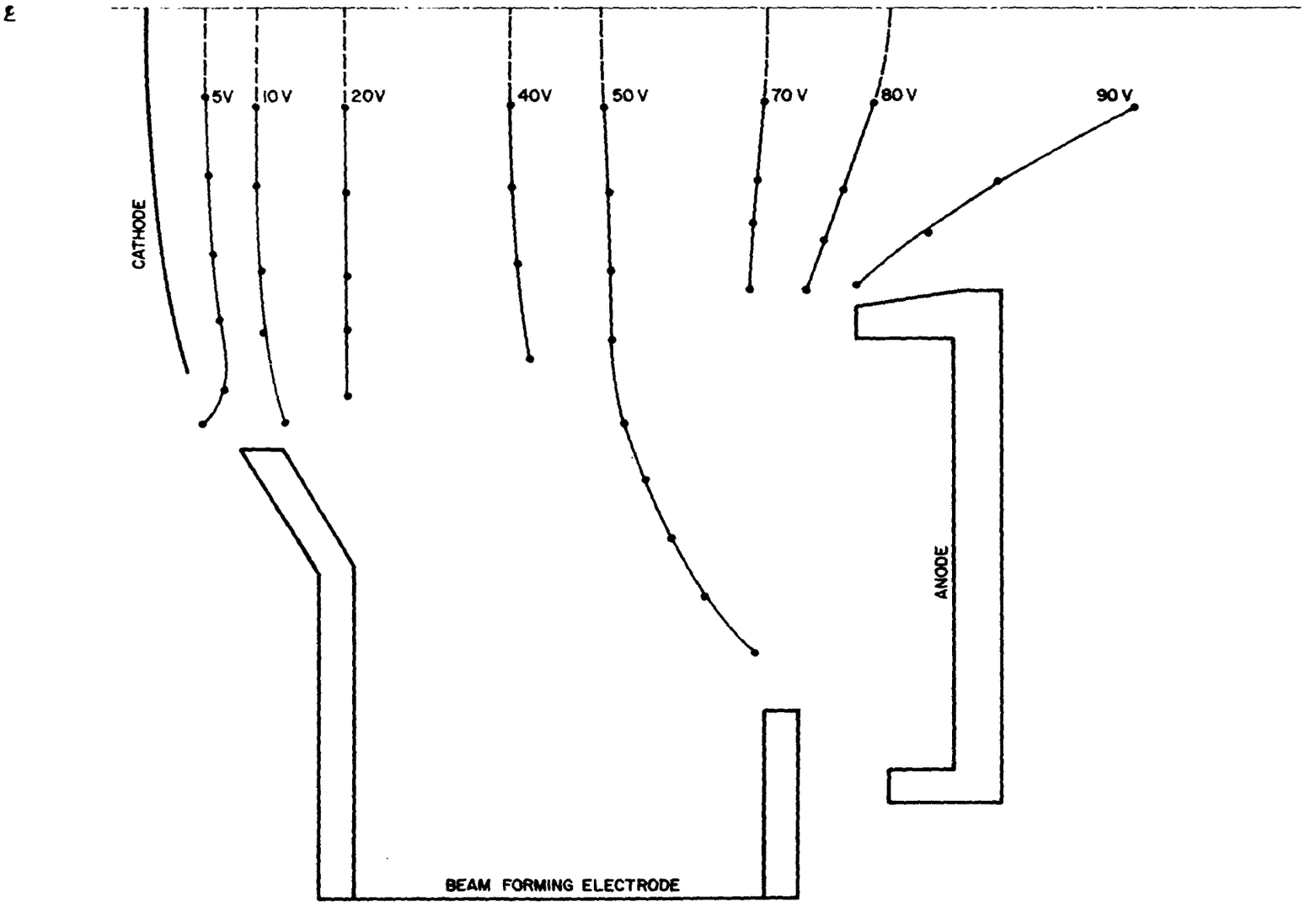

FIG. 8.1 POTENTIAL DISTRIBUTION FOR $P_\mu = 1$ AXIALLY SYMMETRIC ELECTRON GUN. ELECTRODE CONFIGURATION SIMULATED BY METAL ELECTRODES ONLY ON THE UPPER SURFACE OF THE WEDGE.

not correct the error in potential distribution due to wedge thickness. The potential distribution with this modification is shown in Fig. 8.2.

The final step was to approximate the case of embedded electrodes. This was done by drilling holes through the aluminum foil electrodes and the graphite wedge. These holes were coated with silver paint giving the same potential along the hole through the wedge. The potential distribution for this third case is shown in Fig. 8.3.

8.3 Discussion of Results. The potential distribution curves shown in Figs. 8.1 through 8.3 are discussed below for different sections of the electron flow region of the gun.

8.3.1 Cathode Section. Except at the edge of the cathode, the equipotentials in this section show increasing concave (converging) curvature as they pass from Fig. 8.1 through 8.3. A better potential distribution has been obtained which in turn causes a greater converging action upon electron trajectories. But in the region between the edge of the cathode and the beam forming electrode the equipotential takes opposite curvature which causes defocussing action. To avoid this defocussing action at the edge of the cathode, the following suggestions are made.

1. The active area of the cathode should extend only up to the point where the electrons emitted by the cathode do not enter this diverging region. This suffers from the disadvantage that it lowers the perveance of the gun, i.e., decreases the effective emission area of the cathode.
2. The other alternative is to extend the beam forming electrode up to the edge of the cathode and maintain it at the same potential as the cathode. Since there is no opening between

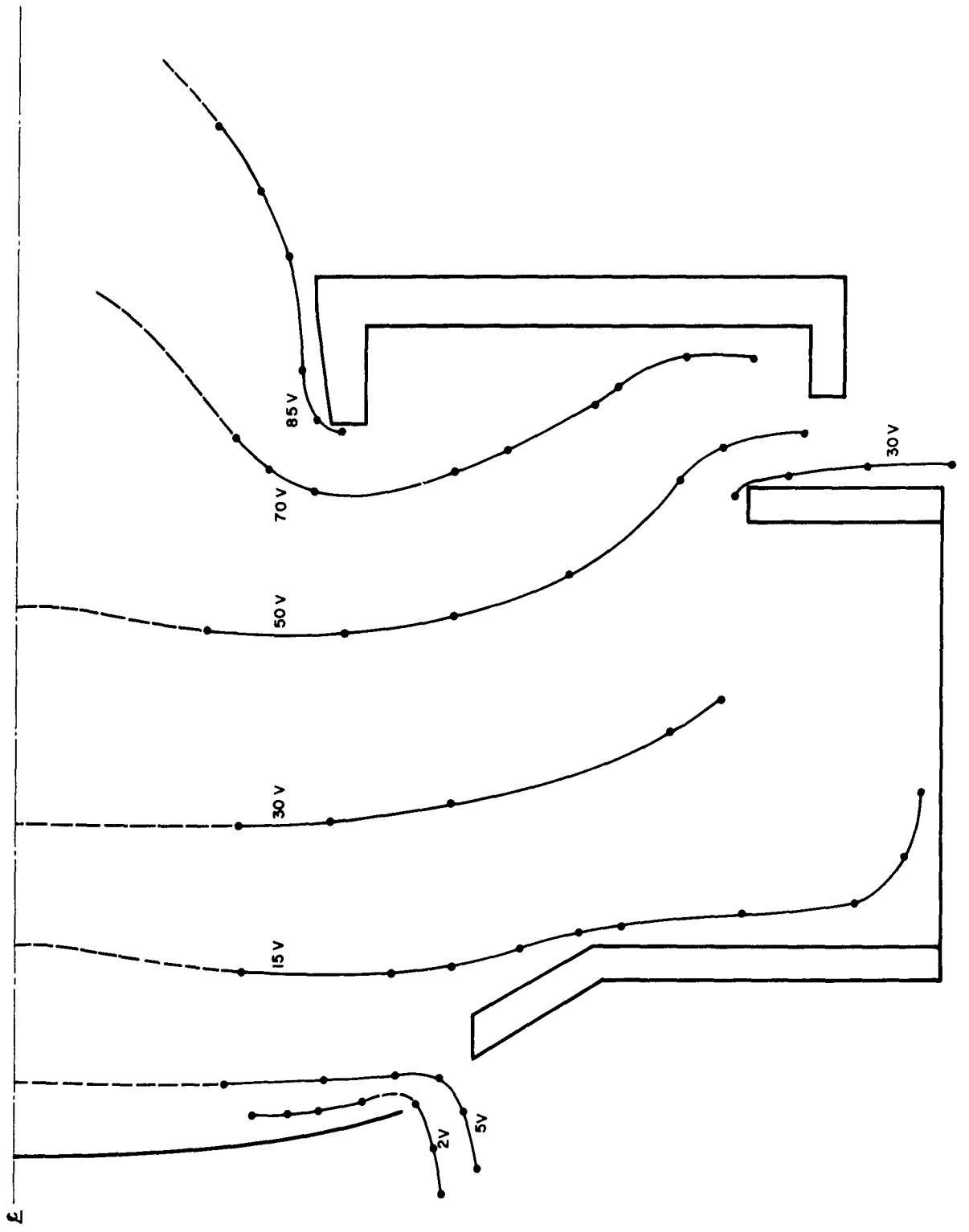

FIG. 8.2 POTENTIAL DISTRIBUTION FOR $P_\mu = 1$ AXIALLY SYMMETRIC ELECTRON GUN. ELECTRODE CONFIGURATION SIMULATED BY ALUMINUM FOIL ELECTRODES ONLY ON THE UPPER SURFACE OF THE WEDGE.

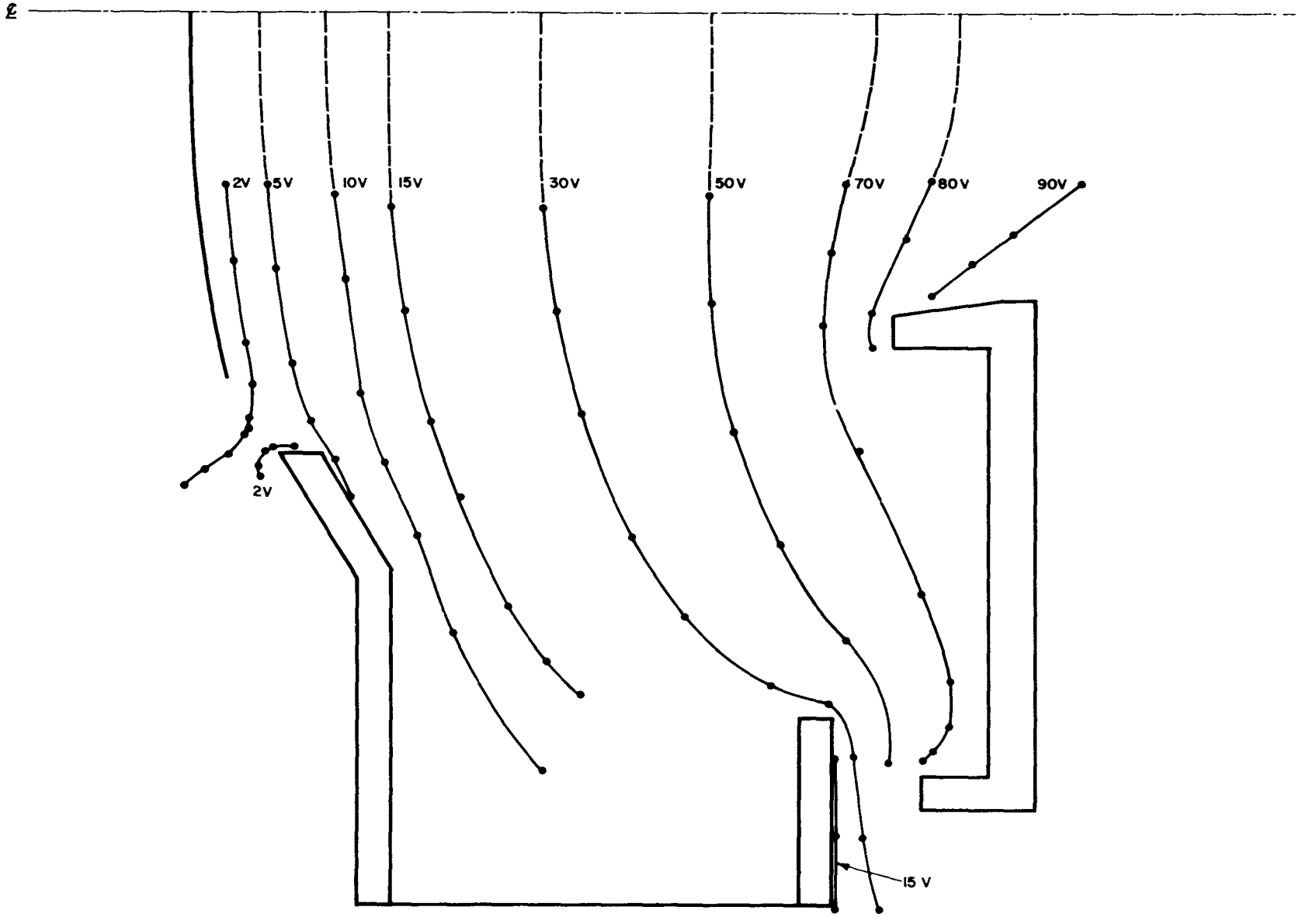

FIG. 8.3 POTENTIAL DISTRIBUTION FOR $P_{\mu} = 1$ AXIALLY SYMMETRIC ELECTRON GUN. ELECTRODE CONFIGURATION SIMULATED BY DRILLING HOLES THROUGH THE ALUMINUM FOIL ELECTRODES AND THE WEDGE AND PAINTING THE SURFACE OF THE HOLES WITH SILVER PAINT.

the edge of the cathode and the beam forming electrode, the potential distribution behind these electrodes will not influence the working region and the diverging action can be avoided without adversely affecting the perveance of the gun.

8.3.2 Middle Section. The potential distribution in the section midway between cathode and anode is also considerably improved in going from Figs. 8.1 to 8.3. The equipotentials shown for this section in Fig. 8.3 possess greater curvature than the other two cases and hence cause greater convergence of the electron trajectories.

Electron trajectories under zero space-charge conditions corresponding to the potential distributions shown in Figs. 8.1 and 8.3 are shown in Figs. 8.4 and 8.5. The greater convergence of trajectories can easily be seen in Fig. 8.5.

It can be concluded that for the case of simulation of gun electrode geometry upon only one surface of the wedge, the proper potential distribution is not well enough reproduced to allow the correct electron trajectories to be obtained. Embedded electrodes should be utilized. The effect of also including gun electrode simulation upon the bottom surface will be studied with the Poisson cell to be used for the study of $P_\mu = 2$ electron guns.

8.4 Other Work. Along with the study of electron gun geometries and electron trajectories, work is continuing on improvement of the electron trajectory calculating system and the linearity of the volume conducting material used for the Poisson cell. To reduce the time required to convert a graphite volume conducting plate into the finished Poisson cell work is being done on a vacuum hold-down as a means of connection of current sources to the base of the graphite plate. This

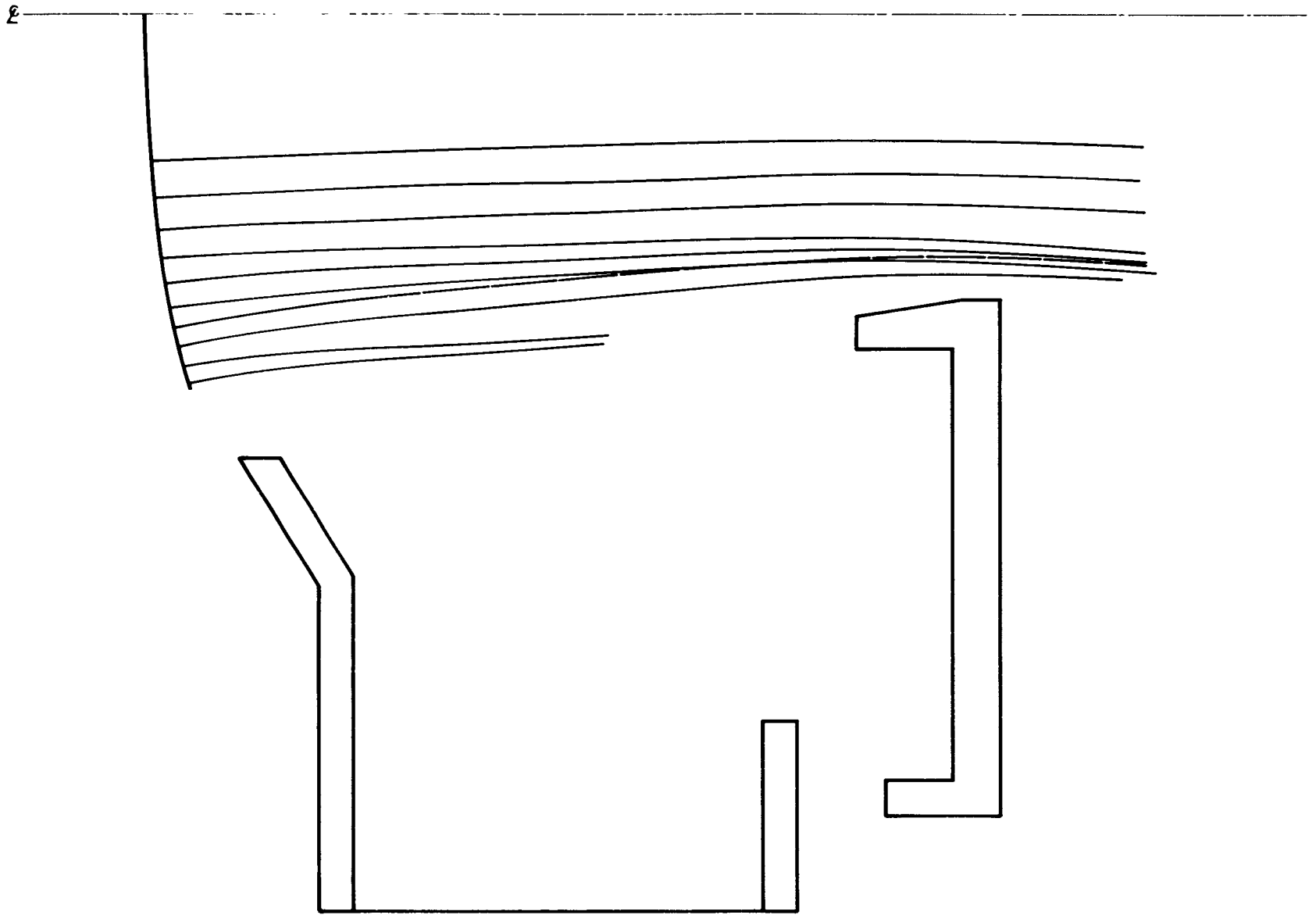

FIG. 8.4 SPACE-CHARGE-FREE TRAJECTORIES FOR $P_\mu = 1$ ELECTRON GUN. ELECTRODE CONFIGURATION SIMULATED BY METAL ELECTRODES ONLY ON THE UPPER SURFACE OF THE WEDGE.

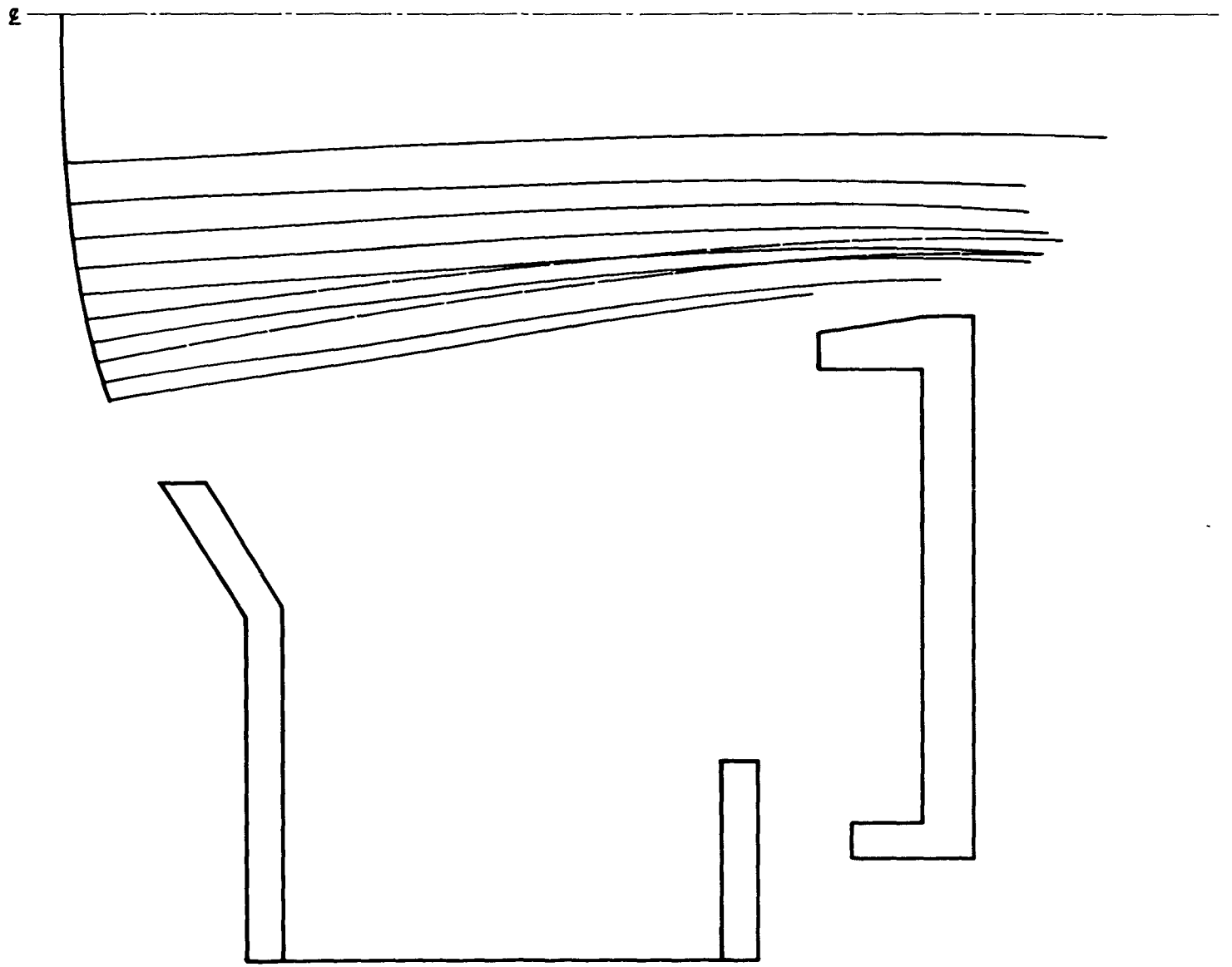

FIG. 8.5 SPACE-CHARGE-FREE TRAJECTORIES FOR $P_\mu = 1$ ELECTRON GUN. ELECTRODE CONFIGURATION SIMULATED BY DRILLING HOLES THROUGH THE ALUMINUM FOIL ELECTRODES AND THE WEDGE AND PAINTING THE SURFACE OF THE HOLES WITH SILVER PAINT.

would eliminate the time previously required to solder and seal the separate sources to the graphite plate. There would be, however, a reduction in the flexibility in the positioning of the current sources.

8.5 Program for the Next Quarter. The electron trajectory configuration for the microperveance-one gun for space-charge-limited operation will be determined. This will require determination of the cathode current emission distribution as well as the proper space-charge distribution. The microperveance-two electron gun will then be studied. The Poisson cell for $P_\mu = 2$ design work is set up to allow simulation of geometries upon the bottom surface of the wedge as well as the top surface. The error in potential distribution for this case will also be examined.

9. Magnetron Injection Gun and High-Power Crestatron (G. T. Konrad)

The type of gun to be used here uses a crossed electric and magnetic field system similar to that of a cylindrical magnetron as illustrated in Fig. 9.1. The only difference is that the electrons are continuously removed from the emitting region by an electric field component in the axial direction. This component is produced by proper shaping of the electrodes near the cathode. The main advantage of this gun is that it has a fairly simple geometry and a dense, hollow electron beam can be obtained from a large cathode emitting surface. In other words, the convergence of the beam can be made large with a simple geometry, while keeping the cathode loading down to a reasonable value. There is reason to believe that the noise properties of this gun will not be similar to those of a magnetron, but rather like the noise in typical guns used in O-type tubes.

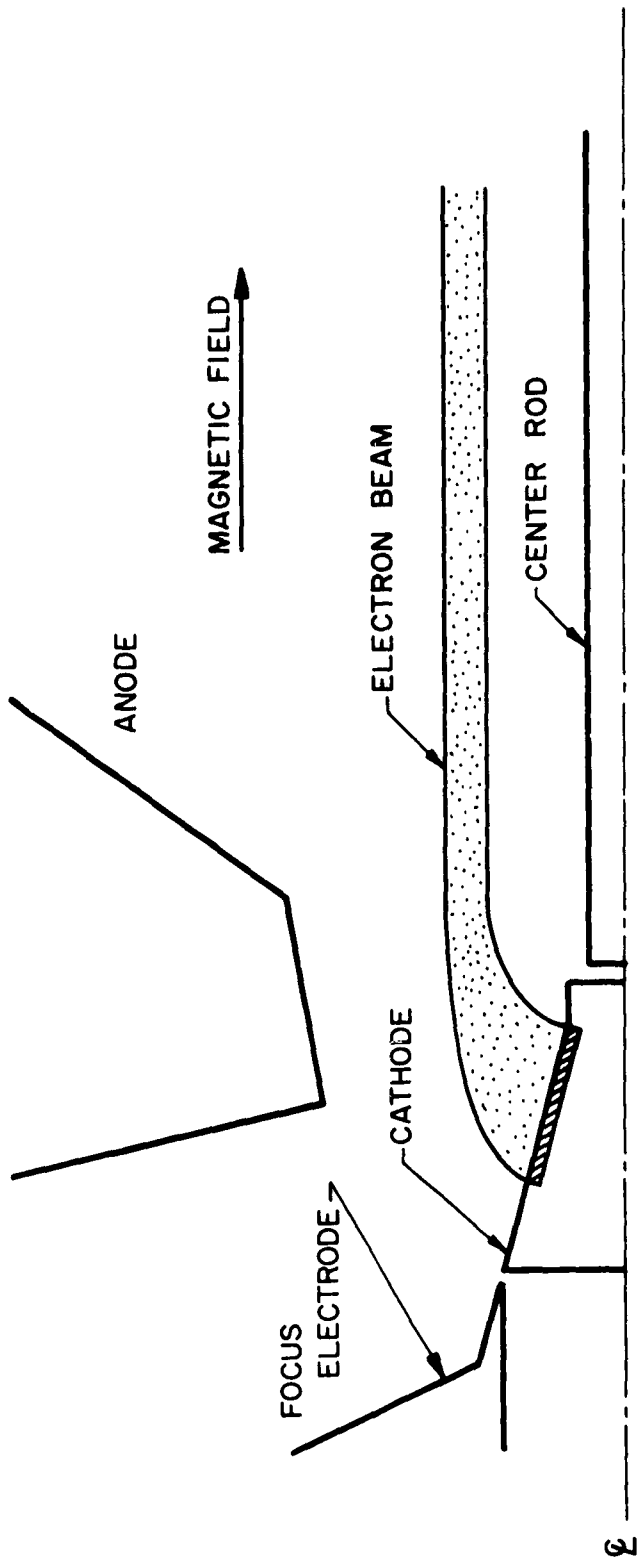

FIG. 9.1 GEOMETRY OF MAGNETRON INJECTION GUN.

A very useful treatment of this gun problem has been given by Waters[1]. Since a cathode design has been derived from this analysis, the correct electrodes will have to be found. One can follow the procedure suggested by Waters or work the problem out by means of an electrolytic tank.

The former method consists of making the approximation that in any plane normal to the axis of the beam, except very close to the cathode, the potential in the charge-free region surrounding the beam varies logarithmically with radius. Since the potential at the beam edge is known from the design curves given by Waters, one can extrapolate logarithmically away from the beam and thus find the potential at any point in the charge-free region near the beam. At any desired potential one may draw smooth curves through the points previously determined. These curves are then the outlines for the electrode shapes. The design by this technique was checked by means of an electrolytic tank, where probes were used to simulate the beam and the electric field near the beam. The agreement between the two methods was excellent. As soon as the parts can be fabricated, a check of this gun will be made in the beam analyzer.

The magnetron injection gun will be used in conjunction with a ring and bar structure. This structure is very similar to those treated by Birdsall and Everhart[2]. The tube will be operated in S-band under a pulsed condition at first. The beam power will be 10 kw peak. It is

---

1. Waters, W. E., "Magnetron Injection Guns--An Exact Theoretical Treatment", TR-843, Diamond Ordnance Fuze Laboratories; April, 1960.

2. Birdsall, C. K., Everhart, T. E., "Modified Contra-Wound Helix Circuits for High-Power Traveling-Wave Tubes", Trans. IRE-PGED, vol. ED-3, pp. 190-204; October, 1956.

anticipated that later in the program a change will be made to cw operation. A BeO envelope will then have to be used in order to keep the r-f structure cool. The r-f power output of the tube could be expected to be 2-3 kw. For proper focusing of the hollow electron beam the magnetic field required in the magnetron injection gun region will be extended over the entire length of the tube.

It is anticipated that the tube will operate in the beating-wave regime at a beam voltage of 18 kv and a beam current of 0.56 amp.

Some of the critical figures and design parameters for the ring and bar structure are shown in Table 9.1 at the center frequency of 3 Gc.

Table 9.1

Data on Ring and Bar Structure

$ka = 0.45$

$\gamma a = 2.0$

velocity parameter, $b = 2.65$

$\frac{v_p}{c} = 0.425$

helix diameter = 0.565 inch

$\frac{\text{helix inner diameter}}{\text{helix outer diameter}} = 0.9$

$\frac{\text{width of ring}}{\text{pitch}} = \frac{1}{8}$

$\frac{\text{width of bar}}{\text{circumference}} = \frac{1}{8}$

calculated interaction impedance $\cong 50\Omega$

gain parameter, $C = 0.07$

A slow-wave structure has been built and was mounted in a glass envelope where it is supported by sapphire rods. Cold tests of this structure are about to be initiated. At the present time it is anticipated that elliptic cavities will be used as transducers between the 50 ohm line and the slow-wave structure. Figure 9.2 gives the critical dimensions of the cold test structure to be tested.

10. Noise Transport in Linear Beam Devices (C. P. Wen)

The outline of two numerical methods for two-dimensional linear beam noise transport analysis was presented in the two previous progress reports respectively. Because of the difficulties developed in the newly installed electronic computer (IBM 709) available on campus, checking out of the programs has been slightly delayed.

10.1 The Monte Carlo Program. The program in which the Monte Carlo techniques are employed to simulate thermionic emission from the cathode may be divided into four parts.

1. For the first two hundred time intervals, random numbers are generated corresponding to proper velocity and current distributions at the cathode surface. Langmuir's one-dimensional space-charge-limited potential distribution is assumed during this period while the diode is being filled with electrons.

2. The d-c potential distribution is computed at the beginning of each time interval by means of the image method for the next two hundred time intervals. Spot checks are made to find out if stable operation conditions are reached for the two-dimensional diode.

3. Current and voltage fluctuations are recorded at various planes parallel to the cathode surface. This part of the program will be run for approximately 3000 time intervals.

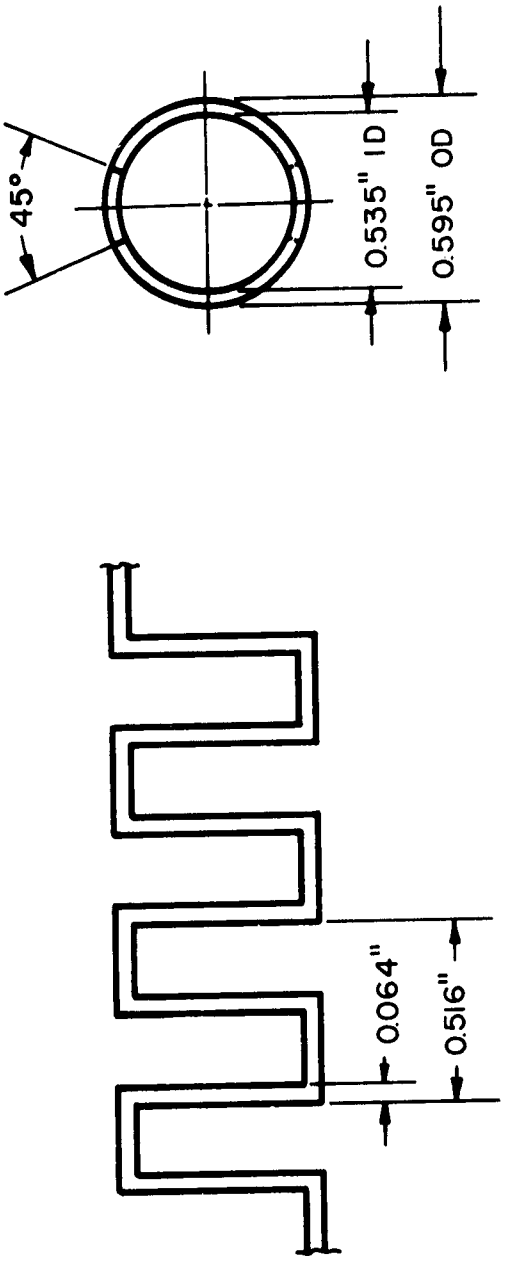

FIG. 9.2 DIAGRAM OF RING AND BAR STRUCTURE FOR HIGH-POWER CRESTATRON.

4. Auto-correlation functions and cross-correlations functions for current and voltage fluctuations are computed from the data from Part 3. The noise parameters and the minimum noise figures are then evaluated by means of Haus' method.

Part 1 of the program has been checked out successfully and test runs are being conducted on Parts 2 and 3. Production runs and evaluation of the data will follow immediately and be discussed in the next progress report.

10.2 The Density Function Method. The density function method program is nearly completed for the analysis of noise propagation in diodes. However, test runs will be held up until the steady-state potential distribution inside the diode is known. Selection of integration steps depends on the location of the reflection points for the velocity classes whose respective velocity parameter w_i is less than zero. It is estimated that the program will be ready in a week or two after Part 2 of the Monte Carlo program is executed.

10.3 K_a-Band Low-Noise Amplifier. Final assembly of the multi-anode low-noise amplifier is underway. A VSWR below 2.5 to 1 for approximately 10 percent bandwidth is obtainable at both matching couplers. The amplifier tube will be ready for evacuation in a few days and experimental investigations will be carried out shortly afterward.

11. Beam-Plasma Interaction Theory (Y. C. Lim)

In the previous report a formal method of solution for the problem of beam-plasma interaction was presented in which an integrating factor of the form $\exp \int(\alpha_i/\mu_i)dz$ occurred. In this section a method of evaluating this factor shall be concisely presented, given the stationary

electric potential $\varphi_e(z)$ and the collision-perturbation coefficient $\alpha_i(z)$ in the finite domain of z, say, in the forms

$$\varphi_e(z) \equiv \sum_{k=1}^{\infty} a_k z^k \quad , \tag{11.1}$$

$$\alpha_i(z) \equiv \sum_{k=0}^{\infty} b_{ik} z^k \quad (i = 1,2,3) \quad , \tag{11.2}$$

where the a_k's are real constants and the b_{ik}'s may be functions of the particle velocity ζ_i. This velocity was also given in the previous report by the equation of constant energy

$$\zeta_i^2 = \zeta_{io}^2 - 2 \frac{Z_i e}{m_i} \varphi_e(z) \triangleq \mu_i^2(z) \quad . \tag{11.3}$$

If it is assumed that the entrance stationary electric field $E_o(0) = -a_1$ does not vanish, then, by Weirstrass' Factorization Theorem, there exists for the velocity function $\mu_i(z)$ one and only one simple root z_o, which is an analytic function of ζ_{io}^2 and hence also of ζ_{io}. It is also clear that z_o is necessarily real, so that the following may be written:

$$\frac{\alpha_i}{\mu_i} = \frac{\alpha_i}{\pm \sqrt{(z-z_o)\, G_i(z,\zeta_{io})}} \quad , \tag{11.4}$$

where G_i is a real entire function of z and ζ_{io} that does not vanish in the finite domain. Thus it is permissible to write, for each i, a power series of the following form

$$\sum_{k=0}^{\infty} c_k z^k = \frac{1}{\sqrt{G_i(z,\zeta_{io})}} \quad , \tag{11.5}$$

where the c_k's (index i being suppressed here for brevity) are either all real or all purely imaginary constants given by the recurrence formula

$$c_n = -\frac{1}{2c_o a_o}\left[\sum_{k=0}^{n-1}\sum_{\ell=0}^{k} c_{k-\ell} c_\ell a_{n-k} + a_o \sum_{\ell=1}^{n-1} c_{n-\ell} c_\ell\right] , \qquad (11.6)$$

with

$$c_o = \frac{\sqrt{-Z_o}}{\zeta_{io}} ,$$

$$c_1 = \frac{\frac{1}{2} m_i \zeta_{io}^2 - Z_i e z_o a_1}{m_i \zeta_{io}^3 \sqrt{-Z_o}} .$$

However, for the ease of evaluating the integral involved in the integrating factor, it is convenient to derive for each of the series Eq. 11.2 and Eq. 11.5 another representation, namely

$$\sum_{k=0}^{\infty} c_k z^k = \sum_{k=0}^{\infty} d_k (z-z_o)^k , \quad \sum_{k=0}^{\infty} b_{ik} z^k = \sum_{k=0}^{\infty} e_k (z-z_o)^k , \qquad (11.7)$$

where naturally

$$d_k = \sum_{\ell=0}^{\infty} \binom{\ell+k}{k} c_{\ell+k} z_o^\ell , \quad e_k = \sum_{\ell=0}^{\infty} \binom{\ell+k}{k} b_{i,\ell+k} z_o^\ell . \qquad (11.8)$$

With these representations, the integrand is simply given by

$$\frac{\alpha_i}{\mu_i} = \pm \frac{d_o c_o}{(z-z_o)^{1/2}} \pm \sum_{j=1}^{\infty}\sum_{k=0}^{j} d_k e_{j-k} (z-z_o)^{j-1/2} , \qquad (11.9)$$

with the plus or minus sign taken according to whether ζ_{io} is positive or negative. The series in the last equation, being uniformly convergent, may be integrated term by term giving

$$\int_{z_o}^{z} \frac{\alpha_i}{\mu_i}\, dz = \pm 2d_o c_o (z-z_o)^{1/2} \pm 2 \sum_{j=1}^{\infty} \sum_{k=0}^{j} d_k e_{j-k} \frac{(z-z_o)^{j+1/2}}{j+1/2} \quad , \quad (11.10)$$

or in terms of coefficients c_k's and $b_{i,j}$'s

$$\int_{z_o}^{z} \frac{\alpha_o}{\mu_i}\, dz = \pm \sum_{j=0}^{\infty} \sum_{n=0}^{\infty} \sum_{k=0}^{j} \sum_{m=0}^{n} \binom{n-m+k}{k} \binom{m+j-k}{j-k}$$

$$\cdot b_{i,m+j-k} c_{n-m+k} z_o^n \frac{(z-z_o)^{j+1/2}}{j+1/2} \quad . \quad (11.11)$$

In all the above formulae z_o denotes the root of $\mu(z)$. This root may be evaluated by the method of indeterminate coefficients. For instance, by setting

$$z_o = \sum_{k=1}^{\infty} A_k (-a_o)^k \quad , \quad (11.12)$$

where

$$a_o \triangleq -\frac{m_i \zeta_{io}^2}{2Z_i e} \quad ,$$

a recurrence formula for the coefficient A_m's can be obtained from the equation $\mu(z_o) = 0$ in the form

$$A_1 = \frac{1}{a_1} \quad , \quad A_m = -\frac{1}{a_m^{(m)}} \sum_{n=1}^{m-1} A_n a_m^{(n)} \quad , \quad (11.13)$$

where

$$a_m^{(n)} \triangleq \sum_{k_{n-1}=n-1}^{m-1} \sum_{k_{n-2}=n-2}^{k_{n-1}-1} \cdots \sum_{k_1=1}^{k_2-1} a_{m-k_{n-1}} a_{k_{n-1}-k_{n-2}} \cdots a_{k_2-k_1} a_{k_1} .$$

With the root z_o completely determined, the integrating factor, $\exp \int(\alpha_i \mu_i)dz$, is shown to be well defined, and may actually be evaluated.

In the next quarterly report an investigation will be made of the ıitions under which an integral equation for the perturbed electric .ield E(z) may be obtained with mathematical rigor.

12. Conclusions (J. E. Rowe)

Experimental data on the variable-pitch helix traveling-wave amplifier indicates that both the small- and large-signal gains and efficiency are enhanced by appropriate pitch variations. The enhanced gain is attributed to increased coupling to the core of the electron beam. Efficiency improvement factors from 1.4 to 2.0 have been obtained on an S-band high-power amplifier. The gain was increased by approximately 3 db.

An elliptic cavity coupler for a traveling-wave amplifier has been demonstrated with an extremely wide bandwidth and a relatively low insertion loss.

Further work on the analysis of noise transport in linear-beam devices and on fundamental beam-plasma interaction theory are discussed.

DISTRIBUTION LIST

No. Copies	Agency
2	Commander, Rome Air Development Center, ATTN: RALTP, Griffiss Air Force Base, New York
1	Commander, Rome Air Development Center, ATTN: RAAP, Griffiss Air Force Base, New York
1	ROAMA (ROZMSTT), Griffiss Air Force Base, New York
1	RADC (RAIS/Mr. Malloy - For Flt Lt. Tanner) Griffiss Air Force Base, New York
1	Signal Corps Liaison Officer, RADC (RAOL, Capt. Norton), Griffiss Air Force Base, New York
1	AFBMD (WDAT-9-24191-0), Air Force Unit Post Office, Los Angeles 45, California
1	AFSC (SCSE), Andrews Air Force Base, Washington 25, D. C.
1	Commander, Air Research and Development Command, ATTN: RDTC, Andrews Air Force Base, Washington 25, D. C.
1	Chief, European Office, Air Research and Development Command, Shell Bldg., 60 Rue Cantersteen, Brussels, Belgium
2	AU (AUL), Maxwell Air Force Base, Alabama
1	Air Force Field Representative, Naval Research Laboratory, ATTN: Code 1010, Washington 25, D. C.
1	AFPR, Lockland Branch, General Electric Company, P. O. Box 91, Cincinnati 15, Ohio
1	Chief, AF Section, MAAG Germany, Box 810, APO 80, New York, New York
1	Chief, Naval Research Laboratory, ATTN: Code 2021, Washington 25, D. C.
1	Chief, Bureau of Ships, ATTN: Code 312, Main Navy Bldg., Washington 25, D. C.
1	Office of the Chief Signal Officer, Department of the Army, ATTN: SIGRD, Washington 25, D. C.
1	Commanding Officer, USASRDL, ATTN: SIGRA/SL-ADT, Fort Monmouth, New Jersey

No. Copies	Agency
1	Director, Signal Corps Engineering Laboratories, ATTN: Thermionics Branch, Evans Signal Laboratory, Belmar, New Jersey
1	ASD(ASAPRD), Wright-Patterson Air Force Base, Ohio
3	Commander, Aeronautical Systems Division, ATTN: WCOSI-3, Wright-Patterson Air Force Base, Ohio
2	Commander, Aeronautical Systems Division, ATTN: WCOSR, Wright-Patterson Air Force Base, Ohio
1	Aeronautical Systems Division, Air Force Systems Command, Wright-Patterson Air Force Base, Ohio, ATTN: Mr. George L. Larr, ASRKSC
1	Dr. Robert T. Young, Chief, Electron Tube Branch, Diamond Ordnance Fuze Laboratories, Washington 25, D. C.
10	ASTIA (TIPCA), Arlington Hall Station, Arlington 12, Virginia
1	Secretariat, Advisory Group on Electron Tubes, 346 Broadway, New York 13, New York
1	Applied Radiation Company, Walnut Creek, California, ATTN: Mr. Neil J. Norris
1	Bell Telephone Laboratories, Murray Hill Laboratory, Murray Hill, New Jersey, ATTN: Dr. J. R. Pierce
1	Bendix Corporation, Systems Planning Division, Ann Arbor, Michigan, ATTN: Technical Library
1	Mr. A. G. Peifer, Bendix Corporation, Research Laboratories, Northwestern Highway and 10-1/2 Mile Road, Detroit 35, Michigan
1	The Electronics Research Laboratory, 427 Cory Hall, The University of California, Berkeley 4, California, ATTN: Mrs. Simmons
1	Prof. R. M. Saunders, University of California, Department of Engineering, Berkeley 4, California
1	Prof. Roy Gould, California Institute of Technology, Department of Electrical Engineering, Pasadena, California
1	Chalmers Institute of Technology, ATTN: Dr. O. E. H. Rydbeck, Research Lab. of Electronics, Gibraltargarten 5 G Gothenberg, Sweden

No. Copies	Agency
1	Prof. W. G. Worcester, University of Colorado, Department of Electrical Engineering, Boulder, Colorado
1	Columbia Radiation Laboratory, Columbia University, 538 West 120th Street, New York 27, New York
1	Prof. L. Eastman, Cornell University, Department of Electrical Engineering, Ithaca, New York
1	Dr. Bernard Arfin, Eitel-McCullough, Inc., San Bruno, California
1	Dr. Donald Preist, Eitel-McCullough, Inc., San Bruno, California
1	University of Florida, Department of Electrical Engineering, Gainesville, Florida
1	Mr. T. Marchese, Federal Telecommunication Laboratories, Inc., 500 Washington Avenue, Nutley, New Jersey
1	Dr. E. D. McArthur, General Electric Company, Electron Tube Division of Research Laboratory, Schenectady, New York
1	Mr. S. Webber, General Electric Microwave Laboratory, 601 California Avenue, Palo Alto, California
1	Harvard University, Cruft Laboratory, Cambridge, Massachusetts, ATTN: Technical Library
1	Mr. James B. Maher, Librarian, R and D Technical Library, Hughes Aircraft Company, Culver City, California
1	Mr. T. Milek, Hughes Aircraft Company, Electron Tube Laboratory, Culver City, California
1	University of Illinois, Department of Electrical Engineering, Electron Tube Section, Urbana, Illinois
1	Dr. D. D. King, John Hopkins University, Radiation Laboratory, Baltimore 2, Maryland
1	Linfield Research Institute, ATTN: Dr. F. Charbonnier, McMinnville, Oregon
1	Dr. Norman Moore, Litton Industries, 960 Industrial Road, San Carlos, California
1	Mr. Robert Butman, Massachusetts Institute of Technology, Lincoln Laboratory, Lexington, Massachusetts

No. Copies	Agency
1	Massachusetts Institute of Technology, Research Laboratory of Electronics, Cambridge 39, Massachusetts, ATTN: Documents Library
1	Microwave Electronics Corporation, 4061 Transport Street, Palo Alto, California, ATTN: Dr. S. F. Kaisel
1	Microwave Associates, ATTN: Dr. P. Chorney, Burlington, Massachusetts
1	Department of Electrical Engineering, University of Minnesota, Minneapolis, Minnesota, ATTN: Dr. W. G. Shepherd
1	N.E.R.A. AS Bergen, Attn: Mr. Erling Illokken, Bergen, Norway
1	Norwegian Defense Research Establishment, ATTN: Dr. Kjell Blotekjaer, Division for Radar, Bergen, Norway
1	Polytechnic Institute of Brooklyn, Documents Library, Brooklyn, New York
1	Mr. W. Teich, Raytheon Manufacturing Company, Spencer Laboratory, Burlington, Massachusetts
1	RCA Laboratories, Princeton, New Jersey, ATTN: Dr. Bernard Hershenov
1	Mr. Hans Jenny, RCA Electron Tube Division, 415 South 5th Street, Harrison, New Jersey
1	Dr. W. M. Webster, Director, Electronic Research Laboratory, RCA Laboratories, Princeton, New Jersey
1	Royal Institute of Technology, ATTN: Dr. Bertil Agdur, Microwave Department, Stockholm 70, Sweden
1	Space Technology Laboratories, ATTN: Dr. I. Kaufman, Canoga Park, California
1	Sperry Corporation, Electronic Tube Division, Gainesville, Florida, ATTN: Mr. P. Bergman
1	Sperry Gyroscope Company, Great Neck, New York, ATTN: Engineering Library
1	Dr. M. Chodorow, Stanford University, Microwave Laboratory, Stanford, California
1	Librarian, Microwave Library, Stanford University, Stanford, California

No. Copies	Agency
1	Dr. D. Goodman, Sylvania Microwave Tube Laboratory, 500 Evelyn Avenue, Mountain View, California
1	Dr. R. G. E. Hutter, Sylvania Electric Products, Inc., Mountain View, California
1	Varian Associates, 611 Hansen Way, Palo Alto, California, ATTN: Technical Library
1	Mr. A. E. Harrison, University of Washington, Department of Electrical Engineering, Seattle 5, Washington
1	Dr. L. A. Roberts, Watkins-Johnson Company, Palo Alto, California
1	Dr. D. A. Watkins, Watkins-Johnson Company, 3333 Hillview Avenue, Palo Alto, California
1	Mr. Shelden S. King, Engineering Librarian, Westinghouse Electric Corporation, P. O. Box 284, Elmira, New York
1	Mr. Gerald Klein, Manager, Microwave Tubes Section, Applied Research Department, Westinghouse Electric Corporation, Box 746, Baltimore 3, Maryland
1	Electronic Technology Laboratory, Aeronautical Systems Division, Wright-Patterson Air Force Base, Ohio, ATTN: ASRNET-1, Lt. E. Champagne
1	Defense Research Member,Canadian Joint Staff, 2450 Massachusetts Avenue, N. W., Washington 8, D. C.
1	Northern Electric Company, Ltd., Research and Development Labs., P. O. Box 3511, Station C, Ottawa, Ontario, Canada

AD_____

The University of Michigan, Electron Physics Laboratory, Ann Arbor, Michigan. THEORETICAL AND EXPERIMENTAL INVESTIGATION OF LARGE-SIGNAL TRAVELING-WAVE TUBES, by C. A. Brackett, S. K. Cho, G. T. Konrad, S. G. Lele, Y. C. Lim, R. J. Martin, J. E. Rowe, C. P. Wen. January, 1962, 36 pp. incl. illus. (Proj. No. 5573, Task No. 55253)

Detailed experimental data on an S-band high-power traveling-wave amplifier with a variable-pitch helix is presented with particular emphasis on the efficiency enhancement achieved across the frequency band. Efficiency improvement factors of from 1.4 to 2 to 1 are demonstrated. The gain is also enhanced over the entire frequency band of operation.

Experimental data on a new elliptic cavity coupler for use with a helical circuit is shown. Low VSWR and insertion loss over a broad frequency band are indicated. The design of a magnetron injection gun for use with a high-power amplifier is outlined. Additional details on the noise transport analyses and beam-plasma interaction theory are given.

UNCLASSIFIED

1. Two-Dimensional Nonlinear Interaction Theory for Klystrons and Traveling-Wave Amplifiers
2. Experiments on Variable-Pitch Helix Traveling-Wave Tubes
3. Beating Wave Klystron
4. Elliptic Cavity Couplers for Traveling-Wave Tubes
5. UHF Crestatron
6. Poisson Cells and Gun Design
7. Magnetron Injection Gun and High-Power Crestatron
8. Noise Transport in Linear Beam Devices
9. Beam-Plasma Interaction Theory

I. Brackett, C. A.
II. Cho, S. K.
III. Konrad, G. T.
IV. Lele, S. G.
V. Lim, Y. C.
VI. Martin, R. J.
VII. Rowe, J. E.
VIII. Wen, C. P.

UNCLASSIFIED

AD_____

The University of Michigan, Electron Physics Laboratory, Ann Arbor, Michigan. THEORETICAL AND EXPERIMENTAL INVESTIGATION OF LARGE-SIGNAL TRAVELING-WAVE TUBES, by C. A. Brackett, S. K. Cho, G. T. Konrad, S. G. Lele, Y. C. Lim, R. J. Martin, J. E. Rowe, C. P. Wen. January, 1962, 36 pp. incl. illus. (Proj. No. 5573, Task No. 55253)

Detailed experimental data on an S-band high-power traveling-wave amplifier with a variable-pitch helix is presented with particular emphasis on the efficiency enhancement achieved across the frequency band. Efficiency improvement factors of from 1.4 to 2 to 1 are demonstrated. The gain is also enhanced over the entire frequency band of operation.

Experimental data on a new elliptic cavity coupler for use with a helical circuit is shown. Low VSWR and insertion loss over a broad frequency band are indicated. The design of a magnetron injection gun for use with a high-power amplifier is outlined. Additional details on the noise transport analyses and beam-plasma interaction theory are given.

UNCLASSIFIED

1. Two-Dimensional Nonlinear Interaction Theory for Klystrons and Traveling-Wave Amplifiers
2. Experiments on Variable-Pitch Helix Traveling-Wave Tubes
3. Beating Wave Klystron
4. Elliptic Cavity Couplers for Traveling-Wave Tubes
5. UHF Crestatron
6. Poisson Cells and Gun Design
7. Magnetron Injection Gun and High-Power Crestatron
8. Noise Transport in Linear Beam Devices
9. Beam-Plasma Interaction Theory

I. Brackett, C. A.
II. Cho, S. K.
III. Konrad, G. T.
IV. Lele, S. G.
V. Lim, Y. C.
VI. Martin, R. J.
VII. Rowe, J. E.
VIII. Wen, C. P.

UNCLASSIFIED

AD___________

The University of Michigan, Electron Physics Laboratory, Ann Arbor, Michigan. THEORETICAL AND EXPERIMENTAL INVESTIGATION OF LARGE-SIGNAL TRAVELING-WAVE TUBES, by C. A. Brackett, S. K. Cho, G. T. Konrad, S. G. Lele, Y. C. Lim, R. J. Martin, J. E. Rowe, C. P. Wen. January, 1962, 36 pp. incl. illus. (Proj. No. 5573, Task No. 55253)

Detailed experimental data on an S-band high-power traveling-wave amplifier with a variable-pitch helix is presented with particular emphasis on the efficiency enhancement achieved across the frequency band. Efficiency improvement factors of from 1.4 to 2 to 1 are demonstrated. The gain is also enhanced over the entire frequency band of operation.

Experimental data on a new elliptic cavity coupler for use with a helical circuit is shown. Low VSWR and insertion loss over a broad frequency band are indicated. The design of a magnetron injection gun for use with a high-power amplifier is outlined. Additional details on the noise transport analyses and beam-plasma interaction theory are given.

UNCLASSIFIED

1. Two-Dimensional Nonlinear Interaction Theory for Klystrons and Traveling-Wave Amplifiers
2. Experiments on Variable-Pitch Helix Traveling-Wave Tubes
3. Beating Wave Klystron
4. Elliptic Cavity Couplers for Traveling-Wave Tubes
5. UHF Crestatron
6. Poisson Cells and Gun Design
7. Magnetron Injection Gun and High-Power Crestatron
8. Noise Transport in Linear Beam Devices
9. Beam-Plasma Interaction Theory

I. Brackett, C. A.
II. Cho, S. K.
III. Konrad, G. T.
IV. Lele, S. G.
V. Lim, Y. C.
VI. Martin, R. J.
VII. Rowe, J. E.
VIII. Wen, C. P.

UNCLASSIFIED

AD___________

The University of Michigan, Electron Physics Laboratory, Ann Arbor, Michigan. THEORETICAL AND EXPERIMENTAL INVESTIGATION OF LARGE-SIGNAL TRAVELING-WAVE TUBES, by C. A. Brackett, S. K. Cho, G. T. Konrad, S. G. Lele, Y. C. Lim, R. J. Martin, J. E. Rowe, C. P. Wen. January, 1962, 36 pp. incl. illus. (Proj. No. 5573, Task No. 55253)

Detailed experimental data on an S-band high-power traveling-wave amplifier with a variable-pitch helix is presented with particular emphasis on the efficiency enhancement achieved across the frequency band. Efficiency improvement factors of from 1.4 to 2 to 1 are demonstrated. The gain is also enhanced over the entire frequency band of operation.

Experimental data on a new elliptic cavity coupler for use with a helical circuit is shown. Low VSWR and insertion loss over a broad frequency band are indicated. The design of a magnetron injection gun for use with a high-power amplifier is outlined. Additional details on the noise transport analyses and beam-plasma interaction theory are given.

UNCLASSIFIED

1. Two-Dimensional Nonlinear Interaction Theory for Klystrons and Traveling-Wave Amplifiers
2. Experiments on Variable-Pitch Helix Traveling-Wave Tubes
3. Beating Wave Klystron
4. Elliptic Cavity Couplers for Traveling-Wave Tubes
5. UHF Crestatron
6. Poisson Cells and Gun Design
7. Magnetron Injection Gun and High-Power Crestatron
8. Noise Transport in Linear Beam Devices
9. Beam-Plasma Interaction Theory

I. Brackett, C. A.
II. Cho, S. K.
III. Konrad, G. T.
IV. Lele, S. G.
V. Lim, Y. C.
VI. Martin, R. J.
VII. Rowe, J. E.
VIII. Wen, C. P.

UNCLASSIFIED

AD___________

The University of Michigan, Electron Physics Laboratory, Ann Arbor, Michigan. THEORETICAL AND EXPERIMENTAL INVESTIGATION OF LARGE-SIGNAL TRAVELING-WAVE TUBES, by C. A. Brackett, S. K. Cho, G. T. Konrad, S. G. Lele, Y. C. Lim, R. J. Martin, J. E. Rowe, C. P. Wen. January, 1962, 36 pp. incl. illus. (Proj. No. 5573, Task No. 55253)

Detailed experimental data on an S-band high-power traveling-wave amplifier with a variable-pitch helix is presented with particular emphasis on the efficiency enhancement achieved across the frequency band. Efficiency improvement factors of from 1.4 to 2 to 1 are demonstrated. The gain is also enhanced over the entire frequency band of operation.

Experimental data on a new elliptic cavity coupler for use with a helical circuit is shown. Low VSWR and insertion loss over a broad frequency band are indicated. The design of a magnetron injection gun for use with a high-power amplifier is outlined. Additional details on the noise transport analyses and beam-plasma interaction theory are given.

UNCLASSIFIED

1. Two-Dimensional Nonlinear Interaction Theory for Klystrons and Traveling-Wave Amplifiers
2. Experiments on Variable-Pitch Helix Traveling-Wave Tubes
3. Beating Wave Klystron
4. Elliptic Cavity Couplers for Traveling-Wave Tubes
5. UHF Crestatron
6. Poisson Cells and Gun Design
7. Magnetron Injection Gun and High-Power Crestatron
8. Noise Transport in Linear Beam Devices
9. Beam-Plasma Interaction Theory

I. Brackett, C. A.
II. Cho, S. K.
III. Konrad, G. T.
IV. Lele, S. G.
V. Lim, Y. C.
VI. Martin, R. J.
VII. Rowe, J. E.
VIII. Wen, C. P.

UNCLASSIFIED

AD___________

The University of Michigan, Electron Physics Laboratory, Ann Arbor, Michigan. THEORETICAL AND EXPERIMENTAL INVESTIGATION OF LARGE-SIGNAL TRAVELING-WAVE TUBES, by C. A. Brackett, S. K. Cho, G. T. Konrad, S. G. Lele, Y. C. Lim, R. J. Martin, J. E. Rowe, C. P. Wen. January, 1962, 36 pp. incl. illus. (Proj. No. 5573, Task No. 55253)

Detailed experimental data on an S-band high-power traveling-wave amplifier with a variable-pitch helix is presented with particular emphasis on the efficiency enhancement achieved across the frequency band. Efficiency improvement factors of from 1.4 to 2 to 1 are demonstrated. The gain is also enhanced over the entire frequency band of operation.

Experimental data on a new elliptic cavity coupler for use with a helical circuit is shown. Low VSWR and insertion loss over a broad frequency band are indicated. The design of a magnetron injection gun for use with a high-power amplifier is outlined. Additional details on the noise transport analyses and beam-plasma interaction theory are given.

UNCLASSIFIED

1. Two-Dimensional Nonlinear Interaction Theory for Klystrons and Traveling-Wave Amplifiers
2. Experiments on Variable-Pitch Helix Traveling-Wave Tubes
3. Beating Wave Klystron
4. Elliptic Cavity Couplers for Traveling-Wave Tubes
5. UHF Crestatron
6. Poisson Cells and Gun Design
7. Magnetron Injection Gun and High-Power Crestatron
8. Noise Transport in Linear Beam Devices
9. Beam-Plasma Interaction Theory

I. Brackett, C. A.
II. Cho, S. K.
III. Konrad, G. T.
IV. Lele, S. G.
V. Lim, Y. C.
VI. Martin, R. J.
VII. Rowe, J. E.
VIII. Wen, C. P.

UNCLASSIFIED